

## Production of $^{61}\text{Cu}$ by $\alpha$ and $^3\text{He}$ Bombardment on Cobalt Target

Yoshio HOMMA and Yukio MURAKAMI\*

*Kyoritsu College of Pharmacy, Shibakoen, Minato-ku, Tokyo 105*

\* *Department of Chemistry, Faculty of Science, Tokyo Metropolitan University, Fukazawa, Setagaya-ku, Tokyo 158*

(Received September 28, 1976)

In order to determine the optimum irradiation conditions to produce the  $^{61}\text{Cu}$  for nuclear medical use, excitation curves and thick-target yield curves were determined for the  $\alpha$  reactions producing  $^{61}\text{Cu}$ ,  $^{57}\text{Co}$ , and  $^{58}\text{Co}$ , and  $^3\text{He}$  reactions producing  $^{61}\text{Cu}$ ,  $^{56}\text{Co}$ ,  $^{57}\text{Co}$ , and  $^{58}\text{Co}$ , both from natural cobalt. The  $^{59}\text{Co}(\alpha, 2n)^{61}\text{Cu}$  and the  $^{59}\text{Co}(^3\text{He}, n)^{61}\text{Cu}$  reactions give cross section peaks of 340 mb and 6 mb at 25 MeV and 35 MeV, respectively. The  $^{61}\text{Cu}$  thick-target yields for these reactions at 40 MeV were 6  $\mu\text{Ci}/\mu\text{Ah}$  and 110  $\mu\text{Ci}/\mu\text{Ah}$ , respectively. A simple and reliable anion-exchange method was developed to provide carrier-free  $^{61}\text{Cu}$ . The purity of  $^{61}\text{Cu}$  was determined with a Ge(Li) spectrometer. Photopeak efficiencies have been calculated at principal  $\gamma$ -ray energies of  $^{61}\text{Cu}$ ,  $^{64}\text{Cu}$ , and  $^{67}\text{Cu}$ , for a 1/2 in. NaI scintillation camera. Alternative nuclear reactions and the methods for producing  $^{61}\text{Cu}$  are compared.

$^{61}\text{Cu}$  has better nuclear properties for use in nuclear medicine.<sup>1)</sup> Its 3.32 h half-life and 284 keV  $\gamma$ -ray make it a particularly useful diagnostic scanning agent giving a much lower absorbed dose for a given count rate than the more readily available  $^{64}\text{Cu}$  and  $^{67}\text{Cu}$ .  $^{61}\text{Cu}$  can be produced with a cyclotron by a  $^{59}\text{Co}(\alpha, 2n)^{61}\text{Cu}$  reaction: this reaction results in a maximum of 6  $\mu\text{Ci}/\mu\text{Ah}$  for 40 MeV  $\alpha$  bombardment.<sup>1)</sup> Bombardment of cobalt has an additional advantage in that the inexpensive monoisotopic element cobalt can be used.

In producing a short-lived radionuclide for use in clinical diagnostic procedures, two factors of prime importance are the yield of the desired nuclide and the degree of contamination with other isotopes, particularly those which have relatively long half-lives and which cannot be separated chemically. To determine the optimum irradiation condition to maximize the yield of the desired nuclide and to minimize the yield of other by-product nuclides, the excitation curves for the reactions concerned must be known.

We have investigated the excitation curves and the thick-target yield curves of  $^{61}\text{Cu}$  and by-product nuclides such as  $^{56}\text{Co}$ ,  $^{57}\text{Co}$ , and  $^{58}\text{Co}$ . Photopeak efficiencies have been calculated at  $\gamma$ -ray energies of these nuclides for sodium iodide crystals. This is of interest in the design of  $\gamma$ -ray taking devices such as a scintillation camera. The information would be of value to users of medical cyclotron interested in the production of  $^{61}\text{Cu}$ .

### Experimental

**Target Preparation.** A thin cobalt target (15—25  $\text{mg}/\text{cm}^2$ ) was electro-deposited from a cobalt sulfate solution ( $\text{CoSO}_4 \cdot 7\text{H}_2\text{O}$  500 g/l,  $\text{NaCl}$  17 g/l,  $\text{H}_3\text{BO}_3$  45 g/l) onto a disk of electrolytic copper foil (35  $\mu$  thick). The electro-deposition was performed at 20—28  $^\circ\text{C}$  in a 30 mm diam cell with a platinum wire anode at the current density of 50  $\text{mA}/\text{cm}^2$  for 170—380 min. After electro-deposition the cobalt foils were carefully removed from the cathode, washed, dried, and weighed. About ten to fifteen foils were stacked on a brass target-holder with water cooled pipes.

**Bombardment.** The stacked target was attached to the beam duct of No. 2 of IPCR cyclotron and bombarded with 0.5—1  $\mu\text{A}$  beam of 40 MeV  $\alpha$  and  $^3\text{He}$  particles. A collimator situated in front of the target reduced the spread in

width of beam to *ca.*  $1.5 \times 1.5 \text{ cm}^2$ . The beam current was measured with a beam current integrator. There was 8% excess in the reading owing to the secondary electrons in the slit edge, the target and of  $\alpha$  and  $^3\text{He}$  particles scattering at the slit edge<sup>2)</sup>. The duration of bombardment was 30—60 min.

**Measurement.** After bombardment,  $\gamma$ -ray spectra of each foil were measured with a 15  $\text{cm}^3$  Ge(Li) detector, which had been accurately calibrated using IAEA  $\gamma$ -ray standard sources. The specific  $\gamma$ -rays and half-lives were sufficiently distinguished without chemical separation. The principal photopeaks of nuclide were followed in order to determine the half-life and confirm the identity of the nuclides. The dead time losses were always less than 10%. For the sake of obtaining better sensitivities the longer-lived nuclides ( $^{56}\text{Co}$ ,  $^{57}\text{Co}$ , and  $^{58}\text{Co}$ ) were analyzed after the decay of  $^{61}\text{Cu}$  was complete. The yields of the nuclides produced in each target were calculated in terms of  $\mu\text{Ci}/\mu\text{Ah}$  at the end of bombardment. The data, foil thickness and the result of beam current measurement were used to calculate the reaction cross sections for all the nuclides observed in each foil. The energy and the intensity of the photopeaks:  $^{61}\text{Cu}$  (284 keV, 12%),  $^{56}\text{Co}$  (847 keV, 100%),  $^{57}\text{Co}$  (122 keV, 87%),  $^{58}\text{Co}$  (810 keV, 99%).

### Results and Discussion

**$\gamma$ -Ray Spectra.** A representative example of the  $\gamma$ -ray spectra is shown in Fig. 1. The upper curve was taken 3.3 h after the end of  $\alpha$  bombardment. The median energy in this foil was 28.8 MeV. The lower curve was taken 6 days after the end of bombardment.  $\gamma$ -Rays from the decay of the longer-lived radionuclide  $^{57}\text{Co}$  can be identified in addition to the 511 keV annihilation quanta from positron emitters such as  $^{61}\text{Cu}$  and  $^{58}\text{Co}$ . No peaks which seem to be due to impurities were observed. The spectra of  $\gamma$ -rays from a  $^3\text{He}$  bombardment foil in which the median  $^3\text{He}$  energy was 38.8 MeV are shown in Fig. 2. In addition to  $\gamma$ -rays from  $^{61}\text{Cu}$ ,  $^{57}\text{Co}$ , and  $^{58}\text{Co}$ , photopeaks from  $^{56}\text{Co}$  can be identified. The  $Q$  values for the nuclear reaction concerned are given in Table 1.

#### Excitation Curves and Thick-target Yield Curves.

**$\alpha$  Reactions:** The yields of  $^{61}\text{Cu}$ ,  $^{57}\text{Co}$ , and  $^{58}\text{Co}$  in each target were calculated in terms of  $\mu\text{Ci}/\mu\text{Ah}$  at the end of bombardment. The reaction cross sections were then calculated by means of the relation:

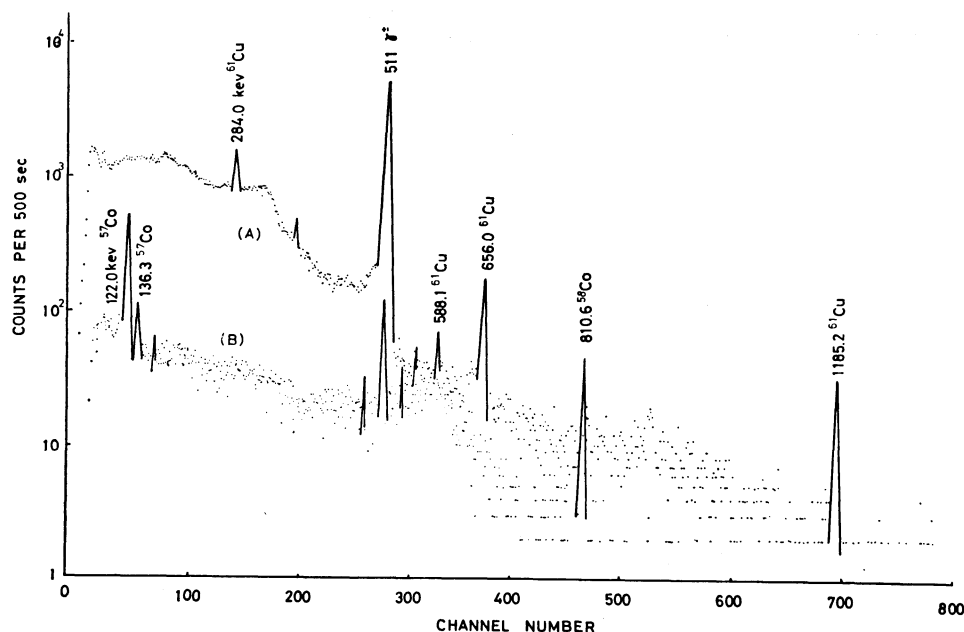


Fig. 1.  $\gamma$ -Ray spectra for  $\alpha$  bombarded target of cobalt. A) taken 3.3 h after bombardment, B) taken 6 d after bombardment.

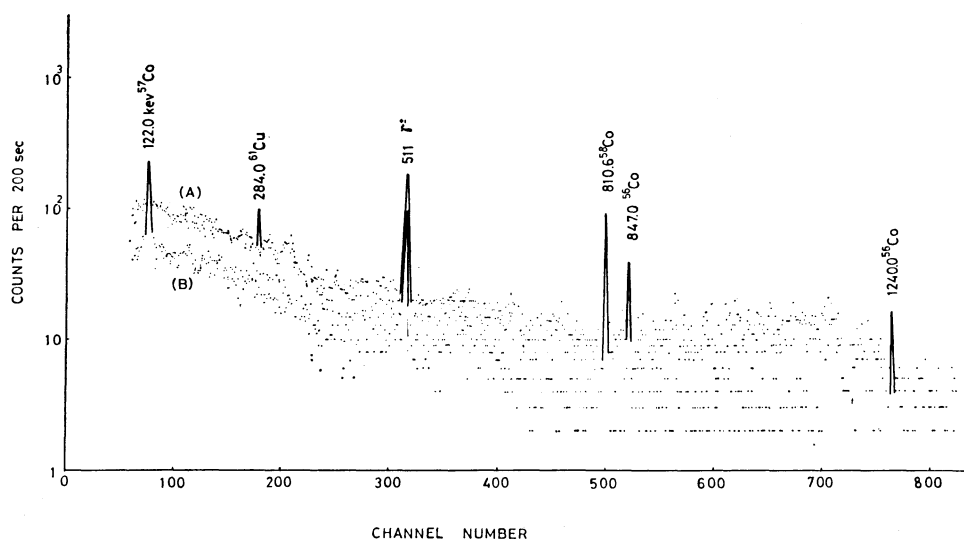


Fig. 2.  $\gamma$ -Ray spectra for  $^3\text{He}$  bombarded target of cobalt. A) taken 3.3 h after bombardment, B) taken 3 d after bombardment.

$$\sigma_E = \frac{A_0}{(1 - e^{-\lambda t}) \cdot N \cdot \phi},$$

where

$\sigma_E$  = the cross section for the reaction at energy  $E$ ,  
 $A_0$  = activity in dps at the end of bombardment,  
 $N$  = number of target nuclei of cobalt target,  
 $\phi$  = particle flux,  
 $\lambda$  = decay constant for the nuclide,  
 $t$  = duration of bombardment.

The excitation curves for the production of  $^{61}\text{Cu}$  by  $\alpha$  bombardment on cobalt are shown in Fig. 3. The maximum cross section of 350 mb is shown at 25 MeV. Above 25 MeV the cross section for  $^{61}\text{Cu}$  production decreases; probably because the  $^{59}\text{Co}(\alpha, xn)^{58}\text{Co}$  and

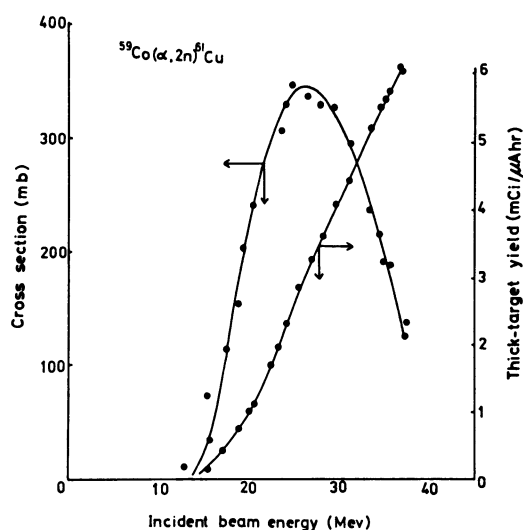
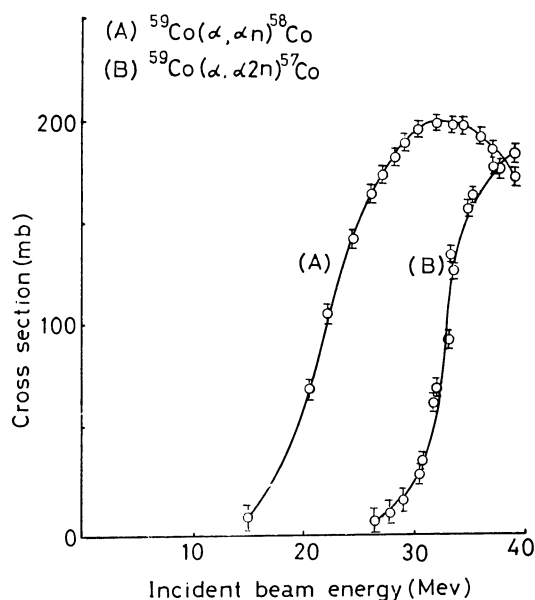
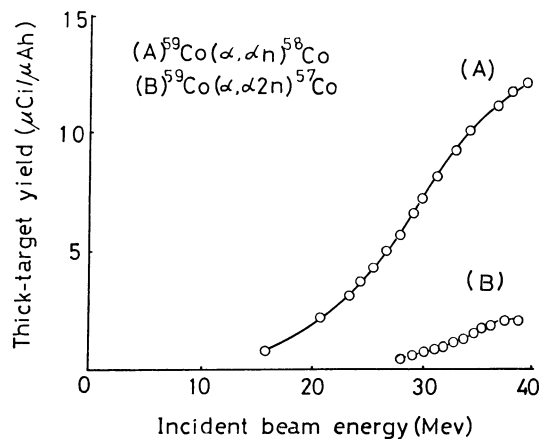
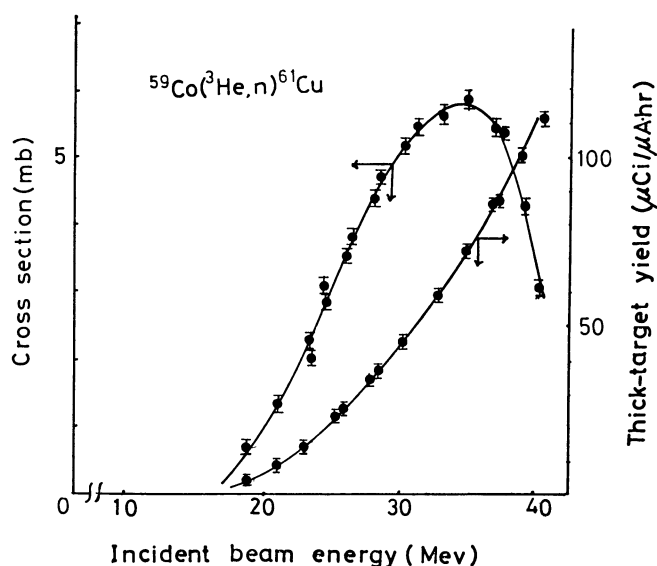
$^{59}\text{Co}(\alpha, \alpha 2n)^{57}\text{Co}$  reactions are more probable than the  $^{59}\text{Co}(\alpha, 2n)^{61}\text{Cu}$  reaction in this energy region (Fig. 4).

The thick-target yield curves were obtained by integrating the thin-target yield *vs.* target depth curves. The thick-target yield curves of  $^{61}\text{Cu}$ ,  $^{57}\text{Co}$ , and  $^{58}\text{Co}$  for  $\alpha$  bombardment of cobalt are given in Figs. 3 and 5.

**$^3\text{He}$  Reactions:** The yields of  $^{61}\text{Cu}$ ,  $^{56}\text{Co}$ ,  $^{57}\text{Co}$ , and  $^{58}\text{Co}$  were calculated in terms of  $\mu\text{Ci}/\mu\text{Ah}$  and the reaction cross sections were calculated exactly in the same way as for the  $\alpha$  particle bombardment described above. The excitation curves for these reactions are plotted in Figs. 6 and 7. The Coulomb barrier for the interaction of  $^3\text{He}$  with  $^{58}\text{Co}$  is about 9.72 MeV, whereas the  $Q$  values for the  $^{59}\text{Co}(^3\text{He}, n)^{61}\text{Cu}$ ,  $^{59}\text{Co}(^3\text{He}, \alpha)^{58}\text{Co}$ ,  $^{59}\text{Co}(^3\text{He}, \alpha n)^{57}\text{Co}$ , and  $^{59}\text{Co}(^3\text{He}, \alpha 2n)^{56}\text{Co}$

TABLE 1.  $\alpha$  AND  $^3\text{He}$  REACTIONS WITH COBALT TARGET

$\alpha$ Reactions		$^3\text{He}$ Reactions	
	Q Value (MeV)		Q Value (MeV)
$^{59}\text{Co}(\alpha, n)^{62}\text{Cu}$	-5.4	$^{59}\text{Co}(^3\text{He}, n)^{61}\text{Cu}$	+6.6
$(\alpha, 2n)^{61}\text{Cu}$	-14.0	$(^3\text{He}, 2n)^{60}\text{Cu}$	-5.1
$(\alpha, 3n)^{60}\text{Cu}$	-25.6	$(^3\text{He}, 3n)^{59}\text{Cu}$	-15.2
$(\alpha, 4n)^{59}\text{Cu}$	-37.7	$(^3\text{He}, 4n)^{58}\text{Cu}$	-27.9
$(\alpha, p)^{62}\text{Ni}$	-0.4	$(^3\text{He}, p)^{61}\text{Ni}$	+9.6
$(\alpha, pn)^{61}\text{Ni}$	-10.9	$(^3\text{He}, pn)^{60}\text{Ni}$	+1.8
$(\alpha, p2n)^{60}\text{Ni}$	-18.7	$(^3\text{He}, p2n)^{59}\text{Ni}$	-9.6
$(\alpha, p3n)^{59}\text{Ni}$	-30.1	$(^3\text{He}, p3n)^{58}\text{Ni}$	-18.6
$(\alpha, \alpha n)^{58}\text{Co}$	-10.4	$(^3\text{He}, \alpha)^{58}\text{Co}$	+10.1
$(\alpha, \alpha 2n)^{57}\text{Co}$	-19.0	$(^3\text{He}, \alpha n)^{57}\text{Co}$	+1.5
$(\alpha, \alpha 3n)^{56}\text{Co}$	-30.4	$(^3\text{He}, \alpha 2n)^{56}\text{Co}$	-9.4
		$(^3\text{He}, \alpha 3n)^{55}\text{Co}$	-19.9

Fig. 3. Excitation curve and thick-target yield curve for  $\alpha$  reaction on cobalt producing  $^{61}\text{Cu}$ .Fig. 4. Excitation curves for  $\alpha$  reaction on cobalt producing  $^{57}\text{Co}$  and  $^{58}\text{Co}$ .Fig. 5. Thick-target yield curves for  $\alpha$  reactions on cobalt producing  $^{57}\text{Co}$  and  $^{58}\text{Co}$ .Fig. 6. Excitation curve and thick-target yield curve for  $^3\text{He}$  reaction on cobalt producing  $^{61}\text{Cu}$ .

reactions are +6.6, +10.1, +1.5, and -9.4 MeV, respectively (Table 1). This indicates that, for the  $^3\text{He}$  particles with sufficient kinetic energy to cross the Coulomb barrier, the cross section for the first reaction is negligibly small.

The  $^{59}\text{Co}(\alpha, 2n)^{61}\text{Cu}$  and the  $^{59}\text{Co}(^3\text{He}, n)^{61}\text{Cu}$  reactions have cross section peaks of 340 and 6 mb at 25 and 35 MeV, respectively. The  $^{61}\text{Cu}$  thick-target yields for these reactions were 6 mCi/ $\mu\text{Ah}$  and 110  $\mu\text{Ci}/\mu\text{Ah}$ , respectively. This shows that  $\alpha$  bombardment is more advantageous than  $^3\text{He}$  bombardment for the production of  $^{61}\text{Cu}$ .

**Chemical Separation and Radionuclidic Purity.** In order to separate  $^{61}\text{Cu}$  from  $^{56}\text{Co}$ ,  $^{57}\text{Co}$ ,  $^{58}\text{Co}$ , and target material, we used the anion-exchange method.<sup>1)</sup> The method has been simplified, with completely satisfactory results, and used for routine production as follows: After 4 h cooling period required to allow the short-lived nuclides such as  $^{60}\text{Cu}$  (23.4 m) and  $^{62}\text{Cu}$  (9.76 m) to decay almost completely, irradiated

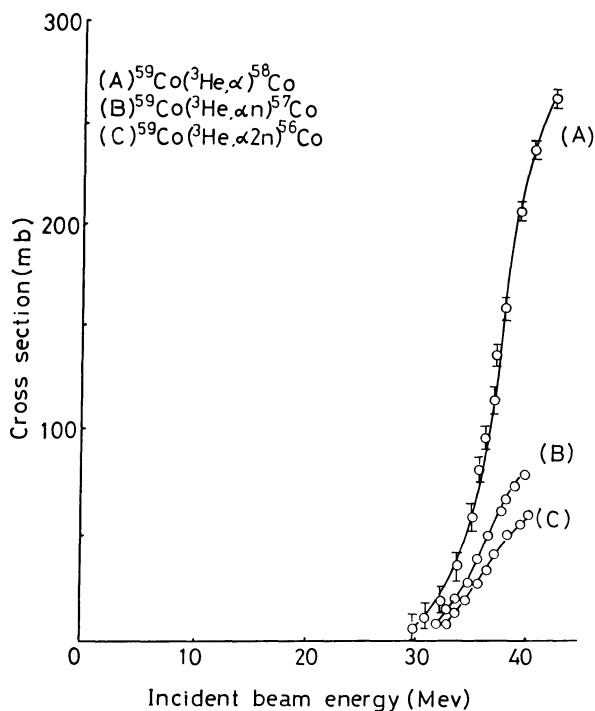


Fig. 7. Excitation curves for  $^3\text{He}$  reactions on cobalt producing  $^{56}\text{Co}$ ,  $^{57}\text{Co}$ , and  $^{58}\text{Co}$ .

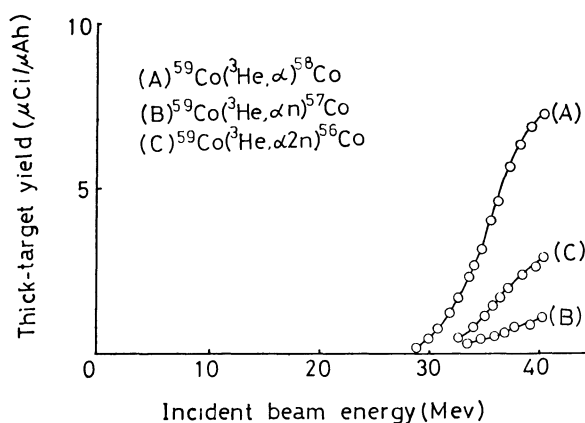


Fig. 8. Thick-target yield curves for  $^3\text{He}$  reactions on cobalt producing  $^{56}\text{Co}$ ,  $^{57}\text{Co}$ , and  $^{58}\text{Co}$ .

cobalt target (150 mg) was dissolved in a mixture of 2 ml of 4M  $\text{HNO}_3$  and a few ml of 6M  $\text{HCl}$  to which a drop of bromine had been added in order to oxidize copper ions. The solution was evaporated nearly to dryness in order to remove excess  $\text{HNO}_3$  and  $\text{Br}_2$ . Twenty-five ml of 8M  $\text{HCl}$  was added to form chloride complexes of  $\text{Cu}^{2+}$  and  $\text{Co}^{2+}$ . The solution was then transferred into a 150 mm  $\times$  13 mm column of Dowex 1-X8 anion-exchanger resin, chloride form, 100–200 mesh. Under these conditions,  $\text{Co}^{2+}$  and  $\text{Cu}^{2+}$  are adsorbed on the resin but not  $\text{Ni}^{2+}$ .<sup>1,4</sup>  $\text{Co}^{2+}$  and  $\text{Cu}^{2+}$  can be eluted from the column with 25 ml of 4M  $\text{HCl}$  and 2M  $\text{HCl}$ , respectively. Carrier-free  $^{61}\text{Cu}$  is recovered as a radionuclidically pure

material in 25 ml of 2M  $\text{HCl}$  solution, which can be easily evaporated to dryness. This makes it possible to convert the tracer into a suitable chemical form. The radiochemical yield was 95%. The procedure is simple, taking less than 150 min. The high radionuclidic purity of  $^{61}\text{Cu}$  attained was determined by  $\gamma$ -ray spectrometry using a  $\text{Ge}(\text{Li})$  detector. No radionuclides of longer-life could be detected.

#### Comparison of Nuclear Reactions for Producing $^{61}\text{Cu}$ .

**Deuteron Bombardment of Natural Zinc Targets:** The thick-target yield of  $^{61}\text{Cu}$  from deuteron bombardment of natural zinc target was ca. 1.2 mCi/ $\mu\text{Ah}$  at 15 MeV.<sup>5</sup> However, the purity of  $^{61}\text{Cu}$  produced by the  $^{64}\text{Zn}(\text{d}, \alpha \text{n})^{61}\text{Cu}$  is restricted by  $^{64}\text{Cu}$  produced by the  $^{66}\text{Zn}(\text{d}, \alpha)^{64}\text{Cu}$ ,  $^{67}\text{Zn}(\text{d}, \alpha \text{n})^{64}\text{Cu}$ , and  $^{64}\text{Zn}(\text{d}, 2\text{p})^{64}\text{Cu}$  reactions and  $^{67}\text{Cu}$  produced by the  $^{68}\text{Zn}(\text{d}, ^3\text{He})^{67}\text{Cu}$  and  $^{67}\text{Zn}(\text{d}, 2\text{p})^{67}\text{Cu}$  reactions. At a bombardment energy of 15 MeV, the maximum levels of  $^{64}\text{Cu}$  and  $^{67}\text{Cu}$  contaminants were 45 and 30%, respectively.

**$^3\text{He}$  Bombardment of Natural Copper Targets:** The maximum cross section for the  $^{63}\text{Cu}(^3\text{He}, \alpha \text{n})^{61}\text{Cu}$  reaction is 88.2 mb at 19.6 MeV, whereas those for the  $^{63}\text{Cu}(^3\text{He}, 2\text{p})^{64}\text{Cu}$  and the  $^{63}\text{Cu}(^3\text{He}, \alpha)^{62}\text{Cu}$  reactions are 126 mb at 21.7 MeV and 42.7 mb at 22.4 MeV, respectively.<sup>6</sup> The results indicate that the purity of  $^{61}\text{Cu}$  produced by this method is not suitable for *in vivo* studies, even if other by-product nuclides such as  $^{65}\text{Ga}$ ,  $^{66}\text{Ga}$ ,  $^{67}\text{Ga}$ ,  $^{62}\text{Zn}$ ,  $^{63}\text{Zn}$ , and  $^{65}\text{Zn}$  are chemically separable.

**Proton Bombardment of Natural Copper Targets:**  $^{61}\text{Cu}$  is also produced by the  $^{63}\text{Cu}(\text{p}, \text{p}2\text{n})^{61}\text{Cu}$  and the  $^{65}\text{Cu}(\text{p}, \text{p}4\text{n})^{61}\text{Cu}$  reactions. A limitation of the above nuclear reactions is that the required particle energies (e.g. 35–60 MeV protons) are not attainable with compact cyclotrons suitable for routine production. Only the cyclotron of the National Institute of Radiological Science can be used. The maximum cross sections for these reactions are approximately 3 times less than that for the  $^{59}\text{Co}(\alpha, 2\text{n})^{61}\text{Cu}$  reaction. The experimental data available show that the maximum cross sections for the  $^{63}\text{Cu}(\text{p}, \text{p}2\text{n})^{61}\text{Cu}$  and the  $^{65}\text{Cu}(\text{p}, \text{p}4\text{n})^{61}\text{Cu}$  reactions are 130 mb at 35 MeV and 100 mb at 60 MeV, respectively.<sup>7</sup> This indicates that the yield of these reactions are not practical for routine production.

**$\alpha$  Bombardment of Enriched Nickel Targets:** A relatively high cross section has been reported for the  $^{58}\text{Ni}(\alpha, \text{p})^{61}\text{Cu}$  reaction which has a maximum value of 310 mb at particle energy 11 MeV.<sup>8</sup> However, the method is not practical, because of the use of a Van de Graaff accelerator and highly enriched nickel isotope (98.4%).

An alternative method was studied in order to obtain  $^{61}\text{Cu}$  by the  $^3\text{He}$  bombardment on natural nickel target. The results of preliminary studies are satisfactory and have advantages over the above mentioned  $^{58}\text{Ni}(\alpha, \text{p})^{61}\text{Cu}$ , primarily because its thick-target yield is 4.9 mCi/ $\mu\text{Ah}$  with  $^3\text{He}$  particle bombardment energy of 40 MeV.<sup>9</sup>

#### Relative Detection Efficiency.

The average absorbed dose delivered to the total body, spleen, kidneys, liver, heart, and brain by  $^{61}\text{Cu}$ ,  $^{64}\text{Cu}$ , and  $^{67}\text{Cu}$  has been calculated.<sup>1</sup> The results show that  $^{61}\text{Cu}$

TABLE 2. PERCENTAGE OF USABLE  $\gamma$ -RAYS OF  $^{61}\text{Cu}$ ,  $^{64}\text{Cu}$ , AND  $^{67}\text{Cu}$ 

Radionuclide	Decay mode	$\gamma$ -Ray		Transmission (%)	Detection efficiency (%)	Usable $\gamma$ -ray (%)
		Energy (MeV)	Intensity (%)			
$^{61}\text{Cu}$ (3.32 h)	$\beta^+$ 60%	0.284	12	62	58	4.3
	$\beta^-$ 30%	0.511	120	63	35	26.5
		1.19	5	53	21	0.5
$^{64}\text{Cu}$ (12.8 h)	$\beta^+$ 19%	0.511	38	63	35	8.3
	$\beta^-$ 38%	1.34	0.5	53	19	0.05
	EC 43%					
$^{67}\text{Cu}$ (61.7 h)	$\beta^-$	0.092	23	53	99	12.1
		0.184	40	59	58	13.7

has the lowest absorbed dose to various organs and tissues. The relative photopeak efficiencies have been calculated at several  $\gamma$ -ray energies of  $^{61}\text{Cu}$ ,  $^{64}\text{Cu}$ , and  $^{67}\text{Cu}$  for a 1/2 in. NaI scintillation camera. The photopeak detection efficiencies for 1/2 in. NaI crystal,<sup>10</sup> intensity<sup>3</sup>) and the tissue attenuation of  $\gamma$ -rays were used to calculate the relative usable  $\gamma$ -ray flux. The results of these calculations are given in Table 2. Usable  $\gamma$ -ray flux from  $^{61}\text{Cu}$  was higher than that from an equal amount of  $^{64}\text{Cu}$ . With the scintillation camera, the 284 keV  $\gamma$ -ray of  $^{61}\text{Cu}$  provides 4.3% usable  $\gamma$ -ray, while the 1340 keV  $\gamma$ -ray of  $^{64}\text{Cu}$  gives as small as 0.05% usable  $\gamma$ -ray. This indicates that the principal  $\gamma$ -ray of  $^{61}\text{Cu}$  (284 keV) is more intense and in an energy range that is more advantageous for scinti-scanning than that of  $^{64}\text{Cu}$ .

On the other hand, five millicuries of  $^{67}\text{Cu}$  is produced by the reaction  $^{68}\text{Zn}(\gamma, p)^{67}\text{Cu}$  for 48 h irradiation of natural zinc in the bremsstrahlung beam from a linear accelerator.<sup>11</sup>  $^{67}\text{Cu}$  has the advantage that the relative detection efficiency for its intense 184 keV  $\gamma$ -ray (40%) is 13.7%. However, its absorbed dose is too high to be used *in vivo* clinical studies,<sup>1</sup> even if high specific activity  $^{67}\text{Cu}$ , having a half-life of 61.7 h, is useful in particularly time consuming biochemical studies.

The 284 keV  $\gamma$ -ray of  $^{61}\text{Cu}$  approaches an optimum energy that is low enough to be efficiently counted with thin NaI crystals allowing use of high resolution collimators, but high enough to obtain necessary tissue penetration. These characteristics make this nuclide highly desirable for nuclear medical application.

### Conclusion

We found the bombardment of cobalt at 40 MeV to be the best method to produce  $^{61}\text{Cu}$  in sufficient quantity for radiopharmaceutical studies. Advantages are the relatively high yield as compared with other

methods, and the high radionuclidic purity of carrier-free  $^{61}\text{Cu}$ . For routine production we have chosen the following bombardment conditions: energy of the incident particles 40 MeV, target thickness 250 mg/cm<sup>2</sup>, beam current 5  $\mu\text{A}$ . The irradiation time varies according to the required quantity of  $^{61}\text{Cu}$  from 1–2 h. Under these conditions, the yield of  $^{61}\text{Cu}$  obtained at the end of 1 and 2 h of bombardment is *ca.* 13 and 26 mCi, respectively, corrected for losses during the course of recovery.

The authors wish to thank Dr. Tadashi Nozaki and members of the cyclotron group of the Institute of Physical and Chemical Research for their valuable discussions and cooperation.

### References

- 1) Y. Homma and Y. Murakami, *Chem. Lett.*, **1976**, 397.
- 2) T. Nozaki, Private communication.
- 3) C. M. Lederer, J. M. Hollander, and I. Perlman, "Table of Isotopes," Wiley, New York (1967).
- 4) K. A. Kraus and G. E. Moore, *J. Am. Chem. Soc.*, **75**, 1460 (1953).
- 5) D. C. Williams and J. W. Irvine, Jr., *Phys. Rev.*, **130**, 265 (1963).
- 6) E. A. Bryant, D. R. F. Cochran, and J. D. Knight, *Phys. Rev.*, **130**, 1512 (1963).
- 7) I. R. Williams and C. B. Fulmer, *Phys. Rev.*, **162**, 1055 (1967).
- 8) F. K. McGowan, P. H. Stelson, and W. G. Smith, *Phys. Rev.*, **133**, B907 (1964).
- 9) E. Shirai, H. Nakahara, and Y. Murakami, Abstr, No. 2S02, National Meeting of the Chemical Society of Japan, Hiratsuka, April 1976.
- 10) H. O. Anger and D. H. Davis, *Rev. Sci. Instrum.*, **35**, 693 (1964).
- 11) N. Marceau, T. P. A. Kruck, D. B. McConnel, and N. Aspin, *Int. J. Appl. Radiat. Isot.*, **21**, 667 (1970).